

Superconductivity from doping Boron icosahedra.

Matteo Calandri

Laboratoire de Minéralogie-Cristallographie, case 115, 4 place Jussieu, 75252, Paris cedex 05, France

Nathalie Vast

Laboratoire des Solides Irradiés, CEA-CNRS-Ecole Polytechnique, 91128 Palaiseau, France

Francesco Mauri

Laboratoire de Minéralogie-Cristallographie, case 115, 4 Place Jussieu, 75252, Paris cedex 05, France

(Dated: February 9, 2019)

We propose a new route to achieve the superconducting state in Boron-rich solids, the hole doping of B_{12} icosahedra. For this purpose we consider a prototype metallic phase of $B_{13}C_2$. We show that in this compound the Boron icosahedral units are the main responsible for the large phonon frequencies logarithmic average, $\langle 65.8 \rangle$ meV, and the moderate electron-phonon coupling $\lambda = 0.8$. We suggest that this high T_c could be a general feature of hole doped Boron icosahedral solids.

PACS numbers: 63.20.Dj, 63.20.Kr, 78.70.Ck, 71.15.Mb

Low atomic number elements have been intensively investigated in the attempt of finding electron phonon mediated superconductors with high critical temperatures (T_c). Boron rich solids are eminent examples. The high energy phonon frequencies of metallic boron layers in the structure of magnesium diboride [1] are the main responsible for the 39 K T_c . Intercalation of these boron layers with lithium and boron substitution with carbon are currently under study [2] in the quest of even higher T_c . Elemental boron becomes metallic (in a non-icosahedral structure [3, 4]) and superconducting at 160 Gpa, with a T_c which increases up to 11.2 K at 250 Gpa [3]. A 23 K T_c has recently been discovered in intermetallic, yttrium palladium boron carbides[5].

High temperature superconductivity has been found in alkali intercalated fullerene (C_{60}) and theoretically suggested in other intercalated carbon polyhedra, C_{20} [6], C_{28} [7] or C_{36} [8]. C_{60} is a band insulator under normal conditions but the intercalation with alkali atoms does generate a metallic state and a consequent superconducting state with T_c up to 40K[9]. Superconductivity is mainly sustained by the high frequency intramolecular phonons so that most of the physical properties of alkali doped fullerenes can be understood from the solid C_{60} electronic and phonon structures. In particular it is seen that the small radius of the molecule substantially increases the electron phonon coupling with respect to the case of the unrolled graphite layer [10]. The study of solids made of light atoms arranged in icosahedral units is then interesting since they can satisfy the two important requirements of having large phonon frequencies and fairly high electron phonon coupling.

In this work we propose a new route to achieve the superconducting state in boron-rich solids, the hole doping of B_{12} icosahedra. For this purpose we consider a prototype metallic phase of $B_{13}C_2$ for which we predict a T_c comparable to that of MgB_2 . We show that in this

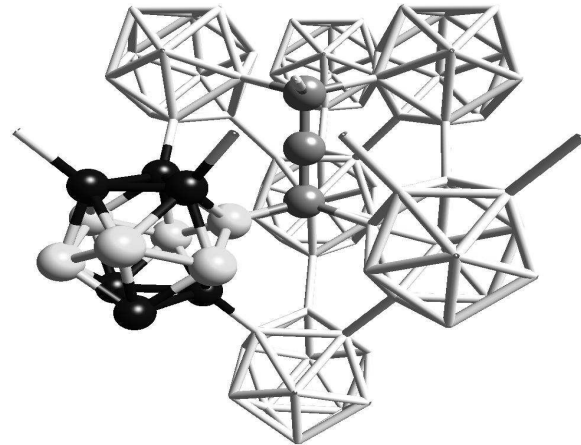


FIG. 1: Atomic structure of $B_{12}C_3$ and of $B_{13}C_2$. The black atoms are the polar sites, bonded to neighboring icosahedra. The white atoms are the equatorial sites. The gray atoms form the chain. In $B_{12}C_3$ the atoms in the chain are CBC and the icosahedra are $B_{11}C$ with the carbon placed in a polar site. In $B_{13}C_2$ the carbon atom in the polar site is replaced with a Boron atom.

compound the boron icosahedral units are the main responsible for the predicted large T_c . Thus this high T_c is a general feature of hole doped boron icosahedral solids.

We consider the hole doping of boron carbide $B_{12}C_3$ (or B_4C), a wide gap band-insulator. Its crystal structure consists of an arrangement of $B_{11}C$ distorted icosahedra on the site of a rombohedral lattice and of a linear C-B-C atom chain [11, 12, 13, 14, 15, 16, 17]. The periodic unit cell contains 15 atoms and is illustrated in fig. 1. Hole doped boron icosahedra can be naturally obtained replacing in $B_{12}C_3$ a boron atom with a carbon, giving $B_{13}C_2$. Due to the carbon substitution there is one hole per unit cell and, $B_{13}C_2$ being non magnetic, band theory predicts a metallic behaviour. At zero temperature

and ambient pressure however, $B_{13}C_2$ is a semiconductor [18]. The insulating character might be related to (i) the presence of structural defects [19, 20] (ii) Mott polaronic features[21]. In the first case a metallic state can be achieved simply by producing high quality samples. In the second case it might be generated by the application of hydrostatic pressure in order to increase the hopping between the icosahedral units. The pressure necessary to metallise $B_{13}C_2$ would be lower than that necessary to metallise $B_{12}C_3$ or α -B. Indeed, the Mott-polaron gap in $B_{13}C_2$ is expected to be much smaller than the several eV gaps of the band insulators $B_{12}C_3$ and α -B.

The two most probable structures of $B_{13}C_2$ are $B_{11}C(BBC)$, *i.e.* $B_{11}C$ icosahedra linked by BBC chains, or $B_{12}(CBC)$, *i.e.* boron icosahedra linked by CBC chains. From the theoretical point of view, Density Functional Theory (DFT) calculations [22] identified the $B_{12}(CBC)$ structure as the most stable one with a 2.09 eV/cell larger binding energy with respect to $B_{11}C(BBC)$. Experimentally [14] the ^{13}C NMR spectrum of $B_{13}C_2$ confirms the DFT calculations. Indeed changing composition from $B_{12}C_3$ to $B_{13}C_2$ the NMR peak associated to the C atom in the icosahedron disappears. Therefore, in this paper, we use the $B_{12}(CBC)$ structure and we refer to it as the $B_{13}C_2$ crystal structure. In other works it has been suggested that the substituted boron is on the chain[23]. We did not consider this proposed structure since we do not expect that the conclusions presented in this work are substantially affected by the location of the additional B atom.

In $B_{13}C_2$ a metallic phase can be achieved either by obtaining clean samples or by applying a small pressure. In DFT, already at room pressure, the ground state is metallic. Therefore we use DFT to study the superconducting properties of the hypothetical metallic state of $B_{13}C_2$. Electronic structure calculations [24] and geometrical optimization are performed using DFT in the local density approximation. We use norm conserving pseudopotentials [25] with a s non local part. The wavefunctions are expanded in plane waves using a 40 Ry cut-off. For the electronic structure we sample the Brillouin zone (BZ) using a 4^3 Monkhorst-Pack grid (10 \mathbf{k} -points in the irreducible BZ wedge) and first order Hermite-Gaussian smearing of 0.03 Ry. From geometrical optimization we obtain the values of $a = 9.686$ (a.u.) and $\alpha = 66.05$ (deg.) for the cell parameters of the rombohedral unit cell, very close to the experimental values [11] ($a = 9.823$ a.u. and $\alpha = 65.62$ deg.).

We calculate the electronic density of states (see fig. 2) at the Fermi level, $N(0)$, of $B_{13}C_2$, using a mesh of $N_k = 14^3$ inequivalent \mathbf{k} -points generated shifting by a random vector the mesh centered at the Γ point. The density of states at the Fermi level is $N(0) = 3.6$ states/eV/unit cell. We decompose the $N(0)$ in icosahedral and chain density of states, by projecting the *ab initio* $B_{13}C_2$ wavefunction on the basis formed by the respective atomic

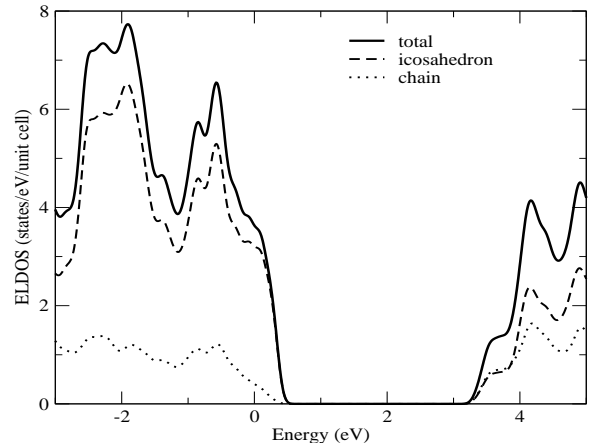


FIG. 2: DFT electronic density of states of $B_{13}C_2$ compared to the icosahedral atoms and chain atoms projected density of states. The energy (eV) is referred to the Fermi energy level.

pseudo-wavefunction (Lowdin population). At the Fermi level the icosahedral states are responsible for 88% of the total density of states ($N_{ico}(0) = 3.2$). In particular the boron atoms in the polar sites have the largest contribution to $N_{ico}(0)$, namely $N_{polar}(0) = 2.3$ and $N_{eq}(0) = 0.9$. Thus, most of the electrons involved in conduction processes resides in icosahedral states and only a small part in chain states, ($N_{chain}(0) = 0.4$).

We compute the harmonic phonon frequencies $\omega_{\mathbf{q},\nu}$ using Density Functional Perturbation Theory in the linear response[24]. We use a $N = 4^3$ Monkhorst-Pack \mathbf{q} -points mesh, \mathbf{q} being the phonon wavevector. The total phonon density of states, $F(\omega)$, together with the phonon density of states restricted to the icosahedral and chain phonon modes are shown in fig. 3.

The icosahedral phonon modes are responsible for most of the weight between 0 and 140 meV. The vibrations of the atoms in the chain explain the high energy feature at 193 meV (both B and C vibrations) and part of the feature at 129 meV (C vibrations). The structures in the chain restricted $F(\omega)$ between 25 and 55 meV are mainly due to B vibrations, while the remaining weight between 60 and 106 meV is due to C vibrations.

The electron phonon interaction for a phonon mode ν with momentum q can be written as:

$$\lambda_{\mathbf{q}\nu} = \frac{4}{\omega_{\mathbf{q}}N(0)N_k} \sum_{\mathbf{k},n,m} |g_{\mathbf{k}n,\mathbf{k}+\mathbf{q}m}^{\nu}|^2 \delta(\varepsilon_{\mathbf{k}n}) \delta(\varepsilon_{\mathbf{k}+\mathbf{q}m}) \quad (1)$$

where the sum is carried out over the BZ, and $\varepsilon_{\mathbf{k}n}$ are the energy bands measured with respect to the Fermi level at point \mathbf{k} . The matrix element is $g_{\mathbf{k}n,\mathbf{k}+\mathbf{q}m}^{\nu} = \langle \mathbf{k}n | \delta V / \delta u_{\mathbf{q}\nu} | \mathbf{k} + \mathbf{q}m \rangle / \sqrt{2\omega_{\mathbf{q}\nu}}$, where $u_{\mathbf{q}\nu}$ is the amplitude of the displacement of the phonon ν of wavevector \mathbf{q} , V is the Kohn-Sham potential and $N(0) = 3.6$ states/eV/unit cell is the electronic DOS at the Fermi

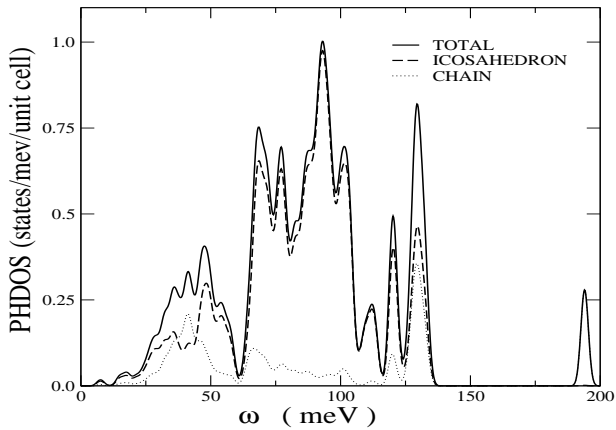


FIG. 3: Phonon density of states, $F(\omega)$, of $B_{13}C_2$. The total density of states (solid line) compared to the phonon density of states of the icosahedral modes (dashed line) and of the chain modes (dotted line). Most of the weight between 0 and 140 meV is due to icosahedral modes.

level. The electron phonon coupling λ is then calculated as an average over the N \mathbf{q} -points mesh and over all the modes, $\lambda = \sum_{\mathbf{q}\nu} \lambda_{\mathbf{q}\nu} / N = 0.81$.

The modes responsible for superconductivity can be identified from the Eliashberg function $\alpha^2 F(\omega)$

$$\alpha^2 F(\omega) = \frac{1}{2N} \sum_{\mathbf{q}\nu} \lambda_{\mathbf{q}\nu} \omega_{\mathbf{q}\nu} \delta(\omega - \omega_{\mathbf{q}\nu}) \quad (2)$$

The Eliashberg function is depicted in fig. 4. Most of the contribution to λ comes from the region from 60 to 105

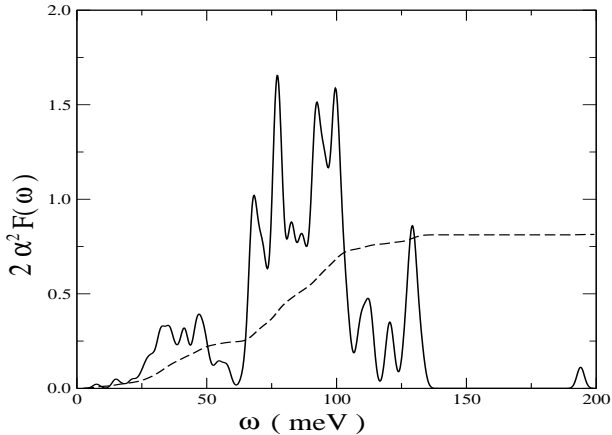


FIG. 4: Eliashberg function (solid line) and average electron phonon coupling (dashed line) of $B_{13}C_2$. The icosahedral phonon modes ranging between 60 and 105 meV give the largest contribution to λ .

The critical superconducting temperature is estimated

from the calculated phonon frequencies and electron phonon coupling using McMillan formula[26]:

$$T_c = \frac{\langle \omega \rangle}{1.2} \exp \left(-\frac{1.04(1+\lambda)}{\lambda - \mu^*(1+0.62\lambda)} \right) \quad (3)$$

where μ^* is the screened Coulomb pseudopotential which takes into account the Coulomb repulsion between the electrons dressed by retardation effects due to the phonons and $\langle \omega \rangle = 65.8$ meV is the phonon frequencies logarithmic average. The calculated values of T_c for $B_{13}C_2$ as a function of μ^* are illustrated in table I. The critical temperature for metallic $B_{13}C_2$ is comparable to the one obtained for MgB_2 and, using McMillan formula, ranges between 15.8 K and 36.7 K.

Material	μ^*	$\langle \omega \rangle$ (meV)	λ	T_c (K)
$B_{13}C_2$	0.1	65.8	0.81	36.7
	0.14	65.8	0.81	27.6
	0.2	65.8	0.81	15.8
MgB_2	0.14	62.0	0.87	30.7

TABLE I: Critical temperatures of $B_{13}C_2$ and MgB_2 . Predicted critical temperatures as a function of the screened Coulomb pseudopotential (μ^*). The critical temperature is estimated using McMillan formula (eq. 3). The results are compared with MgB_2 (from ref. [30]).

In this work we have studied the possible occurrence of superconductivity from hole doping boron icosahedra finding the possibility of having high superconducting critical temperatures. As a possible physical realization of a metallic state we have considered $B_{13}C_2$, which is formed from B_{12} icosahedral units with one hole per icosahedra. Using *ab-initio* calculations we have determined its normal state properties, finding a moderate electron phonon coupling and a large phonon frequencies logarithmic average. We have demonstrated that both properties are connected to the B_{12} building blocks. Indeed the local density of state at the Fermi level and the phonon modes strongly coupled with electrons are localized on the icosahedra. As a consequence our findings are not restricted to $B_{13}C_2$ compounds but can be applied to other metallic compounds composed by B rich icosahedra. For example another possibility to achieve a metallic state is the substitution of P with Si in $B_{12}P_2$ or of As with Si in $B_{12}As_2$. $B_{12}P_2$ and $B_{12}As_2$ are band insulators composed by B_{12} icosahedra and 2-atom P₂ or As₂ chains[23]. The substitution of pentavalent atoms like As and P with a tetravalent Si introduces a hole in the system. $B_{12}P_{2-x}Si_x$ wafer resistivity measurements show a low electrical conductivity [27]. If such conduction is related to bipolaron formation then a metallic state can be achieved applying pressure. An advantage of the 2-atom chain systems ($B_{12}P_{2-x}Si_x$ or $B_{12}As_{2-x}Si_x$) respect to the 3-atom chain systems ($B_{13}C_2$) is the lack

in the formers of an internal soft degree of freedom, the chain bending. Probably this feature makes the 2-atom chain structures more stable under pressure.

We acknowledge illuminating discussion with M. Bernasconi, P. Giannozzi and E. Tosatti. We thank C. J. Pickard for providing us the figure of the molecular structure. Computer time has been granted by IDRIS (project 000544 and 021202). M.C. was supported by a Marie Curie Fellowship of the European Commission, contract No. IHP-HPMF-CT-2001-01185.

[1] Nagamatsu, J., Nakagawa, N., Muranaka, T., Zenitani, Y. & Akimitsu, J., Superconductivity at 39K in magnesium diboride. *Nature (London)* **410**, 63 (2001).

[2] Rosner, H., Kitaigorodsky, A. & Pickett W.E., Prediction of high Tc Superconductivity in hole doped LiBC. *Phys. Rev. Lett.* **88**, 127001 (2002).

[3] Eremets, M.I., Struzhkin, V.V., Mao, H. & Hemley R.J., Superconductivity in boron. *Science* **293**, 272 (2001).

[4] Sanz, D.N., Loubeyre, P. & Mezouar, M., Equation of state and pressure induced amorphization of β -boron from X-ray measurements up to 100 GPa. *Phys. Rev. Lett.* **89**, 245501 (2002).

[5] Cava, R.J., Takagi, H., Batlogg, B., Zandbergen, H.W., Krajewski, J.J., Peck, W.F., van-Dover, R.B., Felder, R.J., Siegrist, T., Mizuhashi, K., Lee, J. O., Eisaki, H., Carter, S. A., Uchida, S., Superconductivity at 23 K in yttrium palladium boride carbide, *Nature* **367** 146 (1994)

[6] Spagnolatti, I., Bernasconi, M. & Benedek, G., Electron phonon interaction in the solid form of the smallest fullerene C_{20} . *Europhys. Lett.* **59**, 572-578 (2002); *ibid* **60**, 329 (2002).

[7] Breda, N., Broglia, R.A., Colò, G., Onida, G., Provati, D. & Vigezzi E., C_{28} : a possible room temperature organic superconductor. *Phys. Rev. B* **62**, 130 (2000).

[8] Collins, P.G., Grossman, J.C., Côté, M., Ishigami, M., Piskoti, C., Louie, S.G., Cohen M.L. & Zettl A., Scanning Tunneling Spectroscopy of C_{36} . *Phys. Rev. Lett.* **82**, 165 (1999).

[9] Gunnarsson, O., Superconductivity in fullerides. *Rev. Mod. Phys.* **69**, 575 (1997).

[10] Schluter, M., Lannoo, M., Needels, M. & Baraff, G.A., Electron phonon coupling and superconductivity in alkali intercalated C_{60} solid. *Phys. Rev. Lett.* **68**, 526 (1992).

[11] Kirfel, A., Gupta, A. & Will, G., The nature of the chemical bonding in boron carbide, $B_{13}C_2$. *Acta Cryst. B* **35**, 1052 (1979).

[12] Larson, A.C., Comments concerning the crystal structure of B_4C . Ref. [28] p. 109. Morosin, B., Aselage, T.L. & Feigelson, R.S., Crystal structure refinements of rhombohedral symmetry materials containing boron-rich icosahedra. *Mater. Res. Soc. Symp. Proc.* **97**, 145 (1987).

[13] Tallant, D.R., Aselage, T.L., Campbell, A.N. & Emin, D., Boron carbide structure by Raman spectroscopy. *Phys. Rev. B* **40**, 5649 (1989).

[14] Kirkpatrick, R.J., Aselage, T., Phillips, B.L. & Montez, B., ^{11}B and ^{13}C NMR spectroscopy of boron carbides. Ref [29] p. 261.

[15] Kuhlmann, U., Werheit, H. & Schwetz, K.A., Distribution of carbon atoms on the boron carbide structure elements. *J. Alloys Compd.* **189**, 249 (1992).

[16] Lazzari, R., Vast, N., Besson, J.M., Baroni, S. & Dal Corso, A., Atomic structure and vibrational properties of icosahedral B_4C boron carbide. *Phys. Rev. Lett.* **83**, 3230 (1999); *ibid* **85**, 4194 (2000).

[17] Mauri, F., Vast, N. & Pickard, C.J., Atomic structure of icosahedral B_4C boron carbide from a first principles analysis of NMR spectra. *Phys. Rev. Lett.*, **87**, 085506 (2001).

[18] Kormann, R. & Zuppiroli, L., Low temperature electronic transport properties of boron carbide. Ref. [28] p.216. Papandreou, N. & Zuppiroli, L., Low temperature AC electrical properties of boron carbide. Ref. [29] p.85.

[19] Favia, P., Stoto, T., Carrard, M., Stadelmann, P.A. & Zuppiroli, L., Order and disorder in boron phases. *Microsc. Microanal. Microstruct.* **7**, 225 (1996). Wei, B., Vajtai, R., Jung, Y.J., Banhart, F., Ramanath, G. & Ajayan, P.M., Massive icosahedral boron carbide crystals. *J. Phys. Chem. B* **106**, 5807 (2002).

[20] Thevenot, F., Boron carbide - a comprehensive review. *J. European Ceramic Society*, **6**, 205 (1990).

[21] Aselage, T. L., Emin, D. & McCready, S.S., Conductivities and Seebeck coefficients of boron carbides: softening bipolaron hopping. *Phys. Rev. B* **64**, 054302 (2001).

[22] Bylander, D. M. & Kleinman, L., Structure of $B_{13}C_2$. *Phys. Rev. B* **43**, 1487 (1991).

[23] Aselage, T.L., Tallant, D.R. & Emin, D., Isotope dependencies of Raman spectra of $B_{12}As_2$, $B_{12}P_2$, $B_{12}O_2$, and $B_{12+x}C_{3-x}$: bonding of intericosahedral chains. *Phys. Rev. B* **56**, 3122 (1997).

[24] Baroni, S., de Gironcoli, S. & Dal Corso, A., Phonons and related crystal properties from density-functional perturbation theory. *Rev. Mod. Phys.* **73**, 515-562 (2001).

[25] Troullier, N. & Martins, J.L., Efficient pseudopotentials for plane-wave calculations. *Phys. Rev. B* **43**, 1993 (1991).

[26] McMillan, W.L., Transition temperature of strong-coupled superconductors. *Phys. Rev.* **167**, 331 (1968).

[27] Kumashiro, Y., Yokohama, T., Sato, K., Ando, Y., Nagatani, S. & Kajiyama, K., Electrical and thermal properties of $B_{12}P_2$ wafers. *J. Solid state Chem.* **154**, 33 (2000).

[28] *Boron-Rich Solids*, edited by Emin, D., Aselage, T.L., Beckel, C.L., Howard, I.A. & Wood, C. (AIP, New York 1986).

[29] *Boron-Rich Solids*, edited by Emin, D., Aselage, T.L., Switendick, A.C., Morosin, B. & Beckel, C.L. (AIP, New York 1991).

[30] Kong, Y., Dolgov, O.V., Jepsen, O. & Andersen O.K., Electron phonon interaction in the normal and superconducting states of MgB_2 . *Phys. Rev. B* **64**, 020501(R) (2001).